Soil CO₂ and O₂ Concentrations Illuminate the Relative Importance of Weathering and Respiration to Seasonal Soil Gas Fluctuations

Caitlin Hodges*

Dep. of Ecosystem Science and Management Pennsylvania State Univ. University Park, PA 16802

Hyojin Kim

Earth and Environmental Systems
Institute and Dep. of Geosciences
Pennsylvania State Univ.
University Park, PA 16802
(current address
Geological Survey of Denmark and
Greenland
Dep. of Quaternary and Groundwater
Mapping
C.F. Møllers Allé 8, Building 1110
8000 Aarhus C, DK)

Susan I. Brantley

Earth and Environmental Systems Institute and Dep. of Geosciences Pennsylvania State Univ. University Park, PA 16802

Jason Kaye

Dep. of Ecosystem Science and Management Pennsylvania State Univ. University Park, PA 16802

Soil CO2 and O2 cycles are coupled in some processes (e.g., respiration) but uncoupled in others (e.g., silicate weathering). One benchmark for interpreting soil biogeochemical processes affected by soil pCO2 and pO2 is to calculate the apparent respiratory quotient (ArQ). When aerobic respiration and diffusion are the dominant controls on gas concentrations, ArQ equals I; ArQ deviates from I when other processes dominate soil CO2 and O2 chemistry. Here, we used ArQ to understand lithologic, hillslope, and seasonal controls on soil gases at the Susquehanna Shale Hills Critical Zone Observatory in central Pennsylvania. We measured soil pCO2 and pO2 at three depths from the soil surface to bedrock across catenas in one shale and one sandstone watershed over three growing seasons. We found that both parent lithology and hillslope position significantly affect soil gas concentrations and ArQ. Soil pCO_2 was highest (>5%) and pO_2 was lowest (<16%) in the valley floors. Controlling for depth, pCO2 was higher and pO2 was lower across all sites in the sandstone watershed. We attribute this pattern to higher macroporosity in sandstone lithologies, which results in greater root respiration at depth. We recorded seasonal variation in ArQ at all sites, with ArQ rising above I during July through September, and dipping below I in the early spring. We hypothesize that this seasonal fluctuation arises from anaerobic respiration in reducing microsites July through September when the soils are wet and demand for O2 is high, followed by oxidation of reduced species when the soils drain and re-oxygenate. We estimate that this anaerobic respiration in microsites contributes 36 g C m⁻² yr⁻¹ to the soil C flux. Our results provide evidence for a conceptual model of metal cycling in temperate watersheds and point to the importance of anaerobic respiration to the carbon flux from forest soils.

Abbreviations: ARQ, apparent respiratory quotient; LRMS, Leading Ridge Midslope; LRRT, Leading Ridge Ridgetop; LRVF, Leading Ridge Valley Floor; NPMS, north planar midslope; SPMS, south planar midslope; SPRT, south planar ridgetop; SPVF, south planar valley floor; SSHCZO, Susquehanna Shale Hills Critical Zone Observatory; TMMS, Tussey Mountain Midslope.

oil CO₂ represents the largest flux of carbon (C) from terrestrial ecosystems, affects carbonate speciation within calcareous soils, and contributes to the acidity that drives silicate weathering (e.g., Amundson et al., 1998; Davidson et al., 1998; Jin et al., 2014). In soils, C resides in both organic and inorganic forms within soil organic matter, biota, minerals, and pore water, with respiration by roots and heterotrophic organisms being the largest flux of C from soils (Chapin et al., 2011). A vast body of past work has described the effects of climate, vegetation, land-scape position, and disturbance history on soil CO₂ production and flux from soils to the atmosphere (e.g., Brook et al., 1983; Hasenmueller et al., 2015; Jarecke et al., 2016; Kaye and Hart, 1998; Sullivan et al., 2008; Riveros-Iregui et al., 2011). These studies have also simplified our interpretations of soil respiration and CO₂ efflux

by neglecting chemical transformations of CO₂ within the soil system (Rey, 2015).

Core Ideas

- Hillslope position and lithology affect soil CO₂ and O₂ in humid temperate forests.
- the ratio of CO₂ and O₂ (ArQ) fluctuates over the growing season.
- the ArQ fluctuations indicate seasonal metal redox cycling at all hillslope positions.
- Anaerobic respiration is important to soil CO₂ flux during the late growing season.

Soil Sci. Soc. Am. J. 83:1167–1180 doi:10.2136/sssaj2019.02.0049 Received 20 Feb. 2019. Accepted I May 2019. *Corresponding author (cah423@psu.edu). © 2019 The Author(s). Re-use requires permission from the publisher.

table I. reactions in soil, with ratio that could result in a change in apparent respiratory quotient (ArQ).

	reaction	CO ₂ /O ₂ ratio	ArQ
Oxidation reactions	4Fe ²⁺ + O ₂ + 4H ₂ O ® 2Fe ₂ O ₃ + 8H ⁺	0:-0.25 per mole Fe	<
	$4Mn^{2+} + 2H_2O + O_2 \otimes 2MnO_2 + 4H$ $NH_4^+ + 2O_2 \otimes NO_3^- + H_2O + 2H^+$	0:-0.25 per mole Mn 0:-2 per mole N	
	2FeS ₂ + 7O ₂ ® 2 Fe ²⁺ + 4 SO ₄ ²⁻	0:-1.75 per mole S	
Carbonate weathering	$CaCO_3 + CO_2 + H_2O $	−I:0 per mole CaCO ₃	<
Silicate weathering	$(Ca, Mg)SiO_3 + CO_2 \otimes (Ca, Mg)CO_3 + SiO_2$	-1:0 per mole silicate mineral	<
CO ₂ equilibrium with soil water	$CO_2 + H_2O \ll H_2CO_3 \ll H^+ + HCO_3^- \ll 2H^+ + CO_3^{2-}$	varies with pH, temperature	< or >
Respiration on C of different oxidation s	states CH ₂ O + O ₂ ® CO ₂ + H ₂ O	I:-I per mole C	I
	2HCOOH + O ₂ ® 2CO ₂ + 2H ₂ O	2:-I per mole C	>
	2CH ₄ O + 3O ₃ ® 2CO ₂ + 4H ₂ O	2:-3 per mole C	<
Anaerobic respiration	$5CH_2O + 4NO_3^- + 4H^+ $	1.25:0 per mole N	>
	$CH_2O + 2MnO_2 + 4H^+ $	0.5:0 per mole Mn	
	$CH_2O + 2Fe_2O_3 + 2H^+ $	0.25:0 per mole Fe	
	$2CH_2O + SO_4^{2-} + 2H^+ R H_2S + 2H_2O + 2CO_2$	2:0 per mole S	
Precipitation of carbonates	$Ca^{2+} + 2HCO_3^{-}$ ® $CaCO_3 + CO_2 + H_2O$	I:0 per mole CaCO ₃	>

Surface flux measurements are insufficient to deconvolute the array of the biotic and abiotic reactions and respiration pathways that potentially add to or subtract from the soil CO₂ pool that diffuses from the soil surface (Angert et al., 2015; Chadwick et al., 1994; Rev. 2015).

For decades both pCO₂ and pO₂ have been measured as a function of depth to understand weathering processes that drive soil formation (Brantley et al., 2014; Holland, 1984; Holland and Zbinden, 1988; Stinchcomb et al., 2018). The capacities of minerals in the parent rock to consume O₂ through oxidation and to consume CO₂ through dissolution have been used to clarify the role of soil gases in weathering induced fracturing and regolith development (Brantley et al., 2014). Recently, scientists interested in understanding biotic controls on soil gases have also started using simultaneous measurements of soil CO₂ and O₂ to calculate the apparent respiratory quotient (Angert et al., 2015; Kim et al., 2017; Sánchez-Cañete et al., 2018; Stinchcomb et al., 2018). The apparent respiratory quotient (ARQ) is the ratio of

change of soil CO₂ from atmospheric conditions divided by the change of soil O₂ from atmospheric concentrations, corrected for the difference in diffusion rates between the two gases. In effect, the ARQ is related to the stoichiometry of the major CO₂ and O₂ reactions in soil, modulated by diffusion. Assuming steady-state conditions with aerobic respiration on a carbohydrate substrate balanced by the resupply of O₂ and loss of CO₂ through diffusion, ARQ should be about 1 (Angert et al., 2015). Indeed, in a meta-analysis of concurrent soil CO₂ and O₂ measurements reported in the literature as a function of depth in temperate forests, Stinchcomb et al. (2018) found that gas diffusion and aerobic respiration dominate in the top 2 m of soils.

Nevertheless, at times the soil system deviates from an ARQ of 1. These deviations are informative; they suggest that other reactions aside from aerobic respiration and diffusion are controlling soil pCO₂ and pO₂ (Table 1; Fig. 1). Deviations of ARQ from 1 can be driven by oxidation of reduced metals in primary minerals (Kim et al., 2017; Stinchcomb et al., 2018), anaerobic

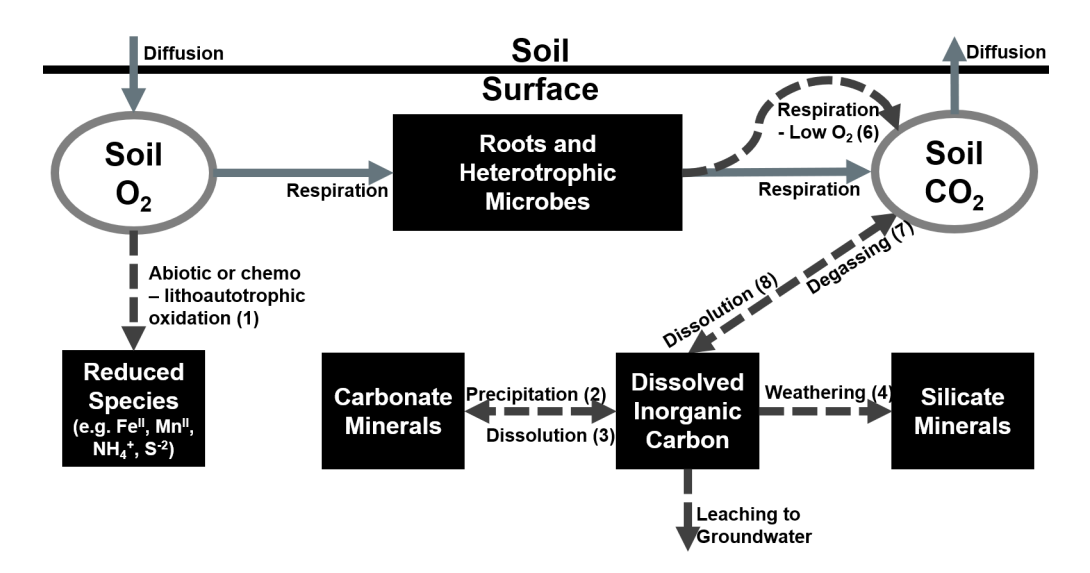


Fig. 1. reactions in the soil system that influence measured pO_2 and pCO_2 . Solid arrows represent processes that occur under theoretical conditions of aerobic respiration and diffusion (apparent respiratory quotient [ArQ] = 1). Dotted lines represent processes that shift ArQ ¹ 1. Numbers in parentheses correspond to the processes that drive deviations in ArQ enumerated in Fig. 2.

respiration by heterotrophs, chemoautotrophy, silicate weathering, carbonate equilibrium (Sánchez-Cañete et al., 2018), or shifts in the dominant C substrate used for respiration (Masiello et al., 2008; Randerson et al., 2006). These controls on ARQ represent chemical and biological processes that may affect estimated rates of soil respiration and regolith weathering (Table 1).

Despite the potential benefits, observations of both soil pCO₂ and pO₂ to enable ARQ estimates with the aim of understanding both abiotic and biotic controls on soil gases are still uncommon. Not much is known of the relative importance of the different mechanisms that drive deviations from the theoretical ARQ. Aside from soil pH (Angert et al., 2015; Ma et al., 2013), landcover type (Angert et al., 2015), and C substrate (Masiello et al., 2008; Randerson et al., 2006), soil physical properties, aspect, and seasonal controls on soil gas ARQ have yet to be explored. Therefore, we sought to identify the landscape and lithologic controls on deviations from the theoretical ARQ in two humid temperate forests. Such an effort to understand how variability of the terrestrial land surface affects biogeochemical and hydrologic fluxes is currently of great interest in the overall effort to upscale watershed models to regional or global scales. In upscaled models, researchers are seeking to understand the importance of rock characteristics, topography, and aspect in governing C and H₂O dynamics (Fan et al., 2019). Toward that goal, we measured pCO₂ and pO₂ within soil profiles in soils across a catena design (Brantley et al., 2016) in one shaleand one sandstone-underlain catchment at the Susquehanna Shale Hills Critical Zone Observatory (SSHCZO) over 2.5 yr. With this observational design, we sought to (i) understand the lithologic controls on soil gas concentrations and ARQ at the SSHCZO, (ii) characterize the variation in soil gas concentrations and ARQ across catena positions and slope aspects, and (iii) identify seasonal patterns in soil gas and ARQ in humid, temperate watersheds. We additionally propose a conceptual model to describe the mechanisms that may underlie observed patterns in ARQ at the SSHCZO.

MAterials AND Methods Field Site Description

Soil gas was sampled and measured at four locations along catenas in both the Shale Hills and Garner Run watersheds of the SSHCZO. The catchments, located within the Ridge and Valley physiographic province, are situated within the Shaver's Creek watershed, less than 5 km apart, and are at about the same elevation of 400 m (Brantley et al., 2016; Li et al., 2018). Mean annual temperature at both sites is 10°C, and mean annual precipitation is 1050 mm.

The Shale Hills watershed of the SSHCZO is a 7.9-ha first-order catchment underlain by the Silurian Rose Hill Shale Formation. The catchment is characterized by steep, planar slopes of 30 to 50 m length dissected by a few concave swales. A first-order intermittent stream that usually dries to disconnected pools in the late summer through fall drains the catchment. Aboveground biomass in Shale Hills is mostly comprised of

oak (Quercus sp.); forest productivity is higher on the southerly aspect slopes and in the valley floors (Smith et al., 2017). Four locations—the valley floor, south midslope, south ridgetop, and north midslope—were chosen for excavation and installation of soil gas wells. The naming of these sites follows the four-letter convention for the SSHCZO established by Jin et al. (2010), so that the first letter represents the north slope (southerly aspect) or south slope (northerly aspect), the second letter represents the type of slope (swale or planar), and the last two letters represent hillslope position (VF, valley floor; MS, midslope; RT, ridgetop). Therefore, the sites we sampled were south planar valley floor (SPVF), south planar midslope (SPMS), south planar ridgetop (SPRT), and north planar midslope (NPMS). Fine-scale soil surveys delineated the soil orders on which the soil gas measurements were made (Lin et al., 2006); the SPVF is mapped as the Ernest series (fine-loamy, mixed, superactive, mesic Aquic Fragiudults), SPMS and SPRT as the Wiekert series (loamy-skeletal, mixed, active, mesic Lithic Dystrudepts), and NPMS as the Berks series (loamy-skeletal, mixed, active, mesic Typic Dystrudepts).

Garner Run is a 134-ha first-order catchment underlain by the Silurian Tuscarora Sandstone Formation. The watershed consists of undissected planar slopes that are 10 times longer and less steep than those in Shale Hills (Brantley et al., 2016; Hoagland et al., 2017; Li et al., 2018). Garner Run is the perennial stream that drains the watershed. Vegetation in Garner Run is different from that in Shale Hills; dominant species in Garner Run are chestnut oak (Quercus prinus Willd.), red maple (Acer rubrum L.), and black birch (Betula lenta L.). Additionally, at Garner Run an understory of mountain laurel (Kalmia latifolia L.), huckleberry (Gaylussacia), and blueberry (Vaccinium sp.) is present. Again, soil pits were excavated and installed with soil gas samplers at the valley floor, south midslope, south ridgetop, and north midslope locations within the watershed. The first two letters of the site names for Garner Run represent the ridges defining the watershed: either Leading Ridge (the south slope, northerly aspect) or Tussey Mountain (the north slope, southerly aspect). The second two letters represent hillslope position. Therefore, the Garner Run sample locations are named Leading Ridge Valley Floor (LRVF), Leading Ridge Midslope (LRMS), Leading Ridge Ridgetop (LRRT), and Tussey Mountain Midslope (TMMS). The LRVF soils are Fine-loamy, mixed, active, mesic Typic Fragiaquults of the Andover Series; the LRMS and TMMS soils are Loamy-skeletal, siliceous, active, mesic Typic Dystrudepts of the Hazleton series; and LRRT are Loamyskeletal, siliceous, active, mesic Typic Dystrudepts of the Dekalb series (Hoagland et al., 2017).

Hand-Sampled Soil Gas Collection and Analysis

Three soil gas samplers at each of three depths were installed at each of the four hillslope locations in the Shale Hills and Garner Run catchments. The gas samplers were installed at 20 cm, 40 cm, and D-20 cm (20 cm above weathered bedrock). The depth to weathered bedrock (D) was defined as the maximum depth that

could be reached with hand tools. The SPRT was only installed with 20 and 40 cm samplers due to shallow bedrock. Hasenmueller et al. (2015) describe soil gas sampler construction and installation in-depth. Briefly, soil gas samplers were constructed of stainless-steel tubing with a stainless-steel mesh affixed to one end. Holes were augered to the desired depth, and the samplers were placed in the hole. Sieved coarse fragments (>2 mm) were installed around the sampler to provide for good air circulation. Sieved soil (<2 mm) was then packed around the sampler above the fragments to the soil surface. The end of the gas access tube exposed to the atmosphere was fitted with a gas-tight three-way lock to prevent atmospheric contamination of soil gas samples.

Soil gas tubes were sampled every 2 wk during spring, summer, and fall from August 2015 through December 2017. Sampling did not take place mid-December through mid-March because soils were saturated or frozen. Air-tight syringes with a one-way lock were used to sample the gas tubes for pCO₂. Prior to sample collection, the 20- and 40-cm access tubes were purged of at least 5 mL gas, and the D-20 was purged of at least 10 mL. After the purge, 5 mL of gas were collected from the 20- and 40-cm wells, and 10 mL of gas were collected from the D-20 wells. Then, 10 mL of soil gas was sampled for pO₂ using a handheld gas analyzer (Model 901, Quantek Instruments). The Quantek 901 has a range of 0 to 100% O₂ and an accuracy of ±0.1% O₂ and was

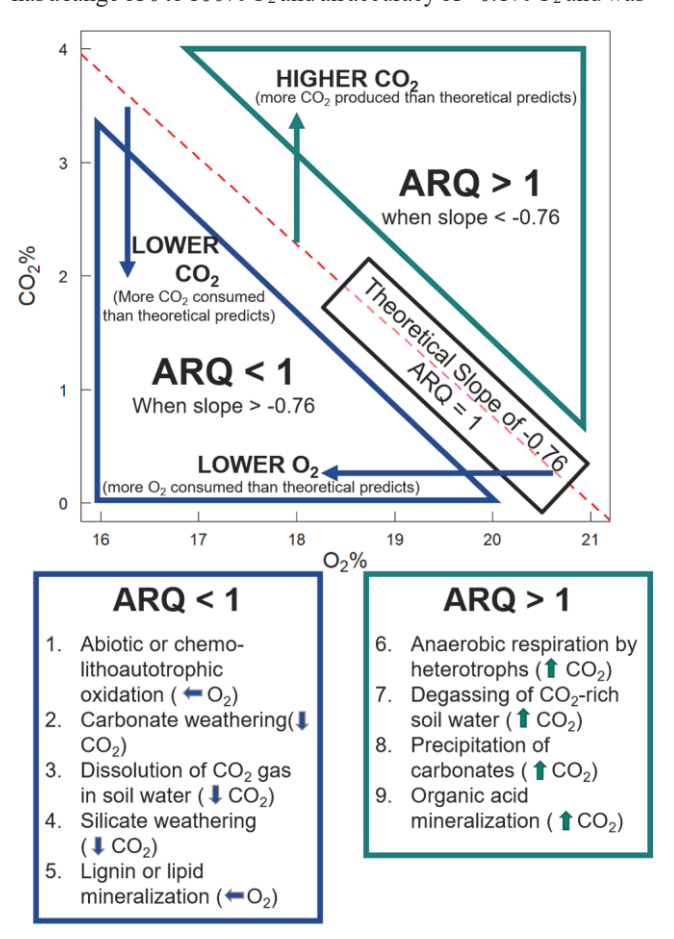


Fig. 2. Conceptual plot of soil pO₂ vs. pCO₂ and potential drivers of deviation from theoretical line governed by diffusion and aerobic respiration on a carbohydrate substrate (i.e., scenarios when apparent respiratory quotient is not 1).

calibrated using O_2 —free gas and ambient air. Assuming an average soil porosity of $0.5~\rm cm^3~\rm cm^{-3}$, the maximum radius of a sphere of soil sampled around the gas well is <6 cm. Three ambient CO_2 samples from about 30 cm above the soil surface were also collected per hillslope position. Soil gas samples were analyzed in the laboratory on a flow-through infrared gas analyzer (LI-7000, LICOR Inc.) within 3 d of collection. Standard curves with 970 and 10,300 ppm CO_2 gas were made to determine sample concentration. Measurement accuracy is within 1% of measured value.

Calculations of ARQ were made following Angert et al. (2015) as shown in Eq. [1].

ARQ =
$$-0.76* \frac{DCO_2}{DO_2}$$
 [1]

where 0.76 is the ratio of the CO₂ and O₂ diffusion coefficients in air (0.138 cm² s⁻¹/0.182 cm² s⁻¹), with the relative effective diffusivity coefficients for both gases cancelling out through division; DCO₂ is the change in soil pCO₂ relative to the atmospheric concentration; and DO₂ is the change in soil pO₂ relative to the atmospheric concentration. To account for the different diffusivities of the gases, all plots of CO₂ vs. O₂ in this manuscript contain a theoretical relationship line with a slope of -0.76 and an x intercept of 20.95 (concentration of O₂ in atmospheric air). Plotting O_2 on the x axis and CO_2 on the y axis is a departure from the convention in some past publications (Kim et al., 2017; Weitzman and Kaye, 2018), but we show it this way to make a direct comparison to ARQ. Plotted in this way, the absolute value of the slope of the regression line for CO2 vs. O2 yields an estimate of the prevailing ARQ at the site. Points that fall above the theoretical line with a slope of -0.76 have an ARQ >1, and points that fall below the theoretical line have an ARQ <1 (Fig. 2).

Soil Gas Sensors at leading ridge Midslope

Soil pCO₂ and pO₂ sensors were installed at 30 and 140 cm in the pit-face of an excavated hole at LRMS in November 2014. Soil pO₂ was sensed by a galvanic cell sensor (SO-400 series, Apogee Instruments), recorded every 15 min, and averaged by day. Apogee sensors were calibrated using O₂ free air and ambient air prior to installation. Sensors can measure O2 concentrations from 0 to 100%, with an accuracy of $\pm 0.1\%$ of O₂ concentration, and a sensor drift of 1 mV a year. Soil pCO₂ was sensed by an optical electrode (Eosense, EosGP) and was also recorded every 15 min and averaged by day. The EosGP sensors were calibrated for 0 to 5000 ppm (0–0.5%) and high 5000 to 50,000 (0.5–5%) CO₂; accuracy is within 1% of recorded ppm. Sensors were connected to a datalogger (CR1000X, Campbell Scientific) for automated recording. The soil O₂ sensor indicates lower concentrations than our hand-sampled data from the same soil depth. We expect that this difference is due to spatial heterogeneity in soil. Because the sensors are physically separated, they likely record conditions of different soil micro-environments, whereas hand-sampled data sample the same soil environment. Furthermore, sensor installation may smear soil and limit gas diffusion to the sensor. Thus, we constrain our interpretation of the sensor data to focus on temporal dynamics of O₂ relative to CO₂. The sensors are ideal for this because they record relative changes in O₂ and CO₂ in the context of precipitation events and changing soil moisture—time scales that are not captured by our hand sampling.

Statistical Analysis

Statistical analyses were performed using SPSS (IBM Corp.) and R (R Core Team, 2018) software. Time series interpolation maps of hand-sampled CO_2 , hand-sampled O_2 , and ARQ from the hand-sampled soil gases were created using the Krig function in the Fields package for R (Nychka et al., 2016), where the soil measurement is plotted over time (x axis) with depth (y axis). All kriged surfaces were created using the same parameters: 1 = 1, q = 50, covariance structure = Mattern. Boundary conditions for the soil surface were set at the measured ambient soil CO_2 concentration for the CO_2 interpolation, 20.95% for the O_2 interpolation, and ARQ = 1 for the ARQ interpolation.

Kriged surfaces were used to visualize variation with time and depth, but we also tested for significant differences of ARQ and gas concentrations by hillslope position, lithology, and season. Lines of best-fit through O₂ vs. CO₂ were generated using the linear modeling (lm) function in R to estimate dominant ARQ (Fig. 2). Slopes were tested for significant differences using ANCOVA (GLM) in SPSS, testing for a significant interaction between hillslope position or lithology with pO₂ on pCO₂. Significant interactions of the independent factors lithology or hillslope position with the covariate (pO₂) indicate signifi-

cantly different slopes. For each hillslope position and lithology, ANCOVA was also performed to test for significantly different slopes by season. April, May, and June were considered spring; July, August, September were considered summer; and October, November, December were considered fall. Finally, ANCOVA was also performed at only the 40-cm sampling depth (the subsurface depth common to all hillslope positions and lithologies) to establish whether the slope of the linear regression at this depth differs significantly as a function of lithology.

A factorial multivariate ANOVA was also performed in SPSS to separately test for the effects of lithology and hillslope position on pO₂ and pCO₂. All data were normally distributed.

rESultS Soil Gas Interpolation of pCO₂, pO₂, and Apparent respiratory Quotient Soil pCO₂

A few overall generalizations can be made about the soil pCO₂ observations. The kriged surfaces indicate that soil pCO₂ varied seasonally, by lithology, with depth, and with hillslope position at the SSHCZO (Fig. 3 and 4). At all hillslope positions on both lithologies, higher pCO₂ was observed at depth. Generally, pCO₂ peaked at all sites in the late summer. In the soil shallower than 40 cm, pCO₂ returned to near-atmospheric concentrations during the winter. When controlling for soil depth differences, pCO₂ was higher at the valley floor positions than at the midslopes and ridgetops throughout the growing season (April

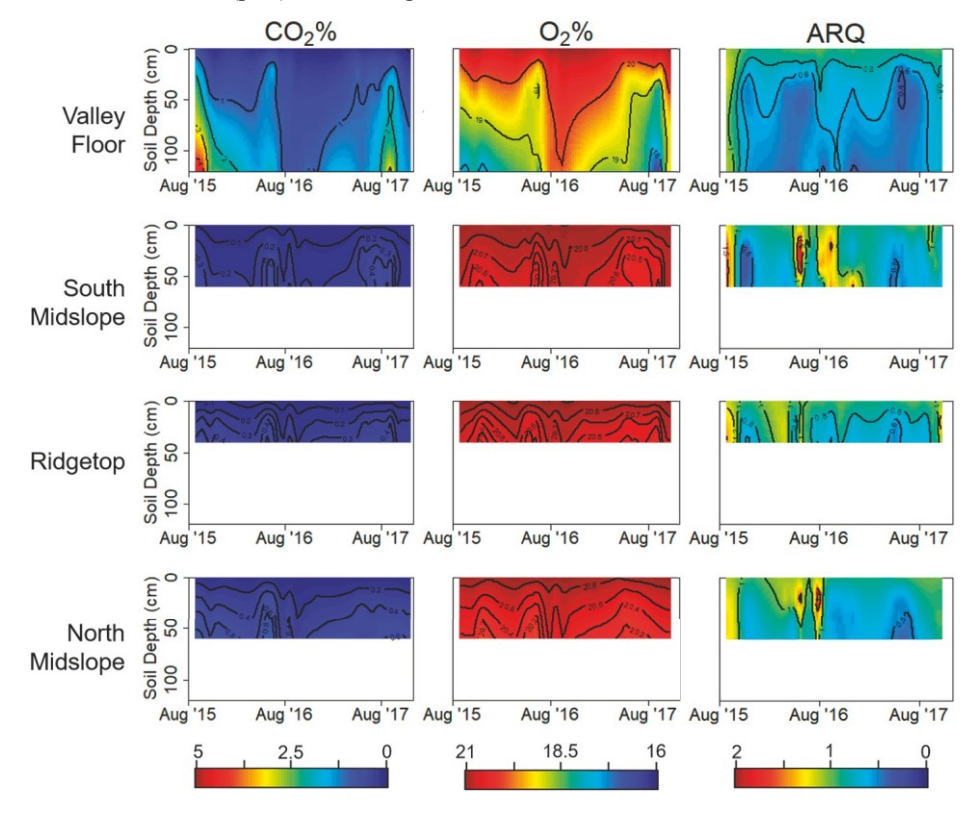


Fig. 3. Interpolated soil pCO₂, pO₂, and apparent respiratory quotient (ArQ) with depth over time for the Shale Hills soil profiles (South Planar Valley Floor [SPVF], South Planar Midslope [SPMS], South Planar ridgetop [SPrt], North Planar Midslope [NPMS]) over the August 2015 to December 2017 sampling periods. Blank spaces represent the difference in depth of augerable soil to bedrock with hillslope position. For the CO₂ column, cooler colors represent gas concentrations closer to atmospheric pCO₂. For the O₂ column, warmer colors represent gas concentrations closer to atmospheric pO₂. In the ArQ column, cool colors represent periods when ArQ <1, and warmer colors represent periods when ArQ >1.

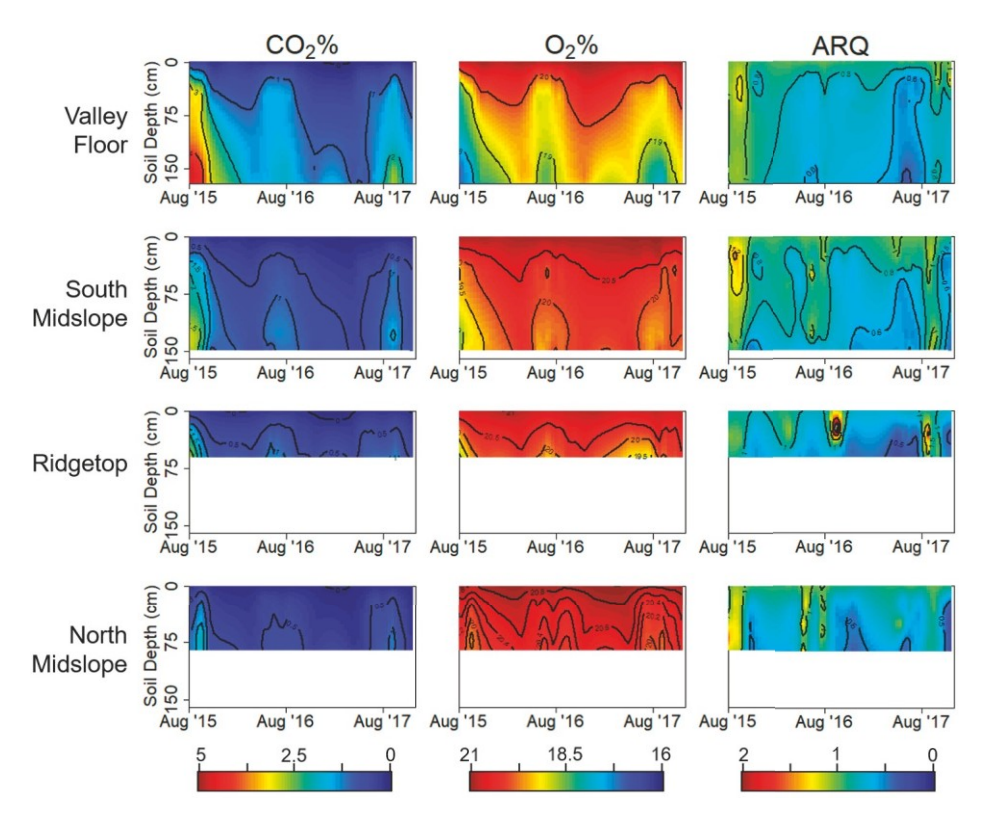


Fig. 4. Interpolated soil pCO₂, pO₂, and apparent respiratory quotient (ArQ) with depth over time for the Garner run soil profiles (leading ridge Valley Floor [IrVF], leading ridge Midslope [IrMS], leading ridge ridgetop [Irrt], tussey Mountain Midslope [tMMS]) over the August 2015 to December 2017 sampling periods. Blank spaces show the difference in depth of augerable soil to bedrock by hillslope position. For the CO₂ column, cooler colors represent gas concentrations closer to atmospheric pCO₂. For the O₂ column, warmer colors represent gas concentrations closer to atmospheric pO₂. In the ArQ column, cool colors represent periods when ArQ <1, and warmer colors represent periods when ArQ >1

through October) on both lithologies (Fig. 3 and 4; Tables 2 and 3). The highest soil pCO₂ (around 5%) was observed at the D-20 depth at the valley floor positions of both Shale Hills and Garner Run, although average soil pCO₂ was higher at the valley floor of Garner Run (1.70 \pm 0.07%) than Shale Hills (1.24 \pm 0.06%) over all measurements (p < 0.001) (Tables 2 and 3). Differences between the lithologies were even more marked in shallow soils; the south midslope and ridgetop attained higher soil pCO₂ concentrations at comparable depths in the late growing season at Garner Run (south midslope avg., 0.98 \pm 0.04%; ridgetop avg., 0.96 \pm 0.04%) (Table 3; Fig. 4) than at Shale Hills (south midslope avg., 0.27 \pm 0.01%; ridgetop avg., 0.33 \pm 0.01%) (Table 3; Fig. 3).

Soil pO₂

The lowest soil pO_2 (about 16-17%) was recorded in the late summer, and the highest (close to atmospheric concentrations) was recorded in the winter (Fig. 3 and 4). At all hillslope positions and lithologies, lower pO_2 was observed at depth. Soil pO_2 was lower at the valley floor positions of Shale Hills and Garner Run

table 2. Multivariate ANOVA results testing the effects of lithology and Hillslope position on soil pO_2 and pCO_2 .

		pCO_2		pO_2	
	df	F	p Value	F	p Value
Lithology	- 1	229.69	<0.0001	167.51	<0.0001
Hillslope position	3	200.5	<0.0001	432.92	<0.0001
Hillslope position × Lithology	3	18.67	<0.0001	37.691	<0.0001
Error	2265				

than the midslopes and ridgetop throughout the growing season (Tables 2, 3). Interestingly, whereas pCO_2 was higher at Garner Run than Shale Hills in the valley floor position (p < 0.05), pO_2 is not different between the two valley floors (Table 3). However, the south midslope and ridgetop recorded lower pO_2 at Garner Run than Shale Hills, mirroring the higher pCO_2 at Garner Run than Shale Hills (Tables 2, 3). This is true even at comparable depths at the midslope and ridgetop positions (Fig. 3 and 4).

table 3. Means \pm SE and tukey honestly significant difference groupings for the interaction of lithology by hillslope position on both CO₂ and O₂.

	pCO_2	pO_2		
	9	- %		
Shale Hills				
Valley Floor	$1.24 \pm 0.06b \dagger$	19.40 ± 0.06d		
South midslope	$0.27 \pm 0.01f$	20.64 ± 0.01a		
Ridgetop	$0.33 \pm 0.01ef$	$20.60 \pm 0.01a$		
North midslope	0.48 ± 0.02 de	$20.42 \pm 0.02b$		
Garner Run				
Valley floor	1.70 ± 0.07a	19.30 ± 0.05d		
South midslope	$0.98 \pm 0.04c$	$20.03 \pm 0.03c$		
Ridgetop	0.96 ± 0.04c	19.98 ± 0.03c		
North midslope	$0.59 \pm 0.02d$	20.37 ± 0.02b		
L.M. Salt all	2.1 1:00	. 1		

[†] Means within the same column with different letters are significantly different (p < 0.05).

Shale Hills

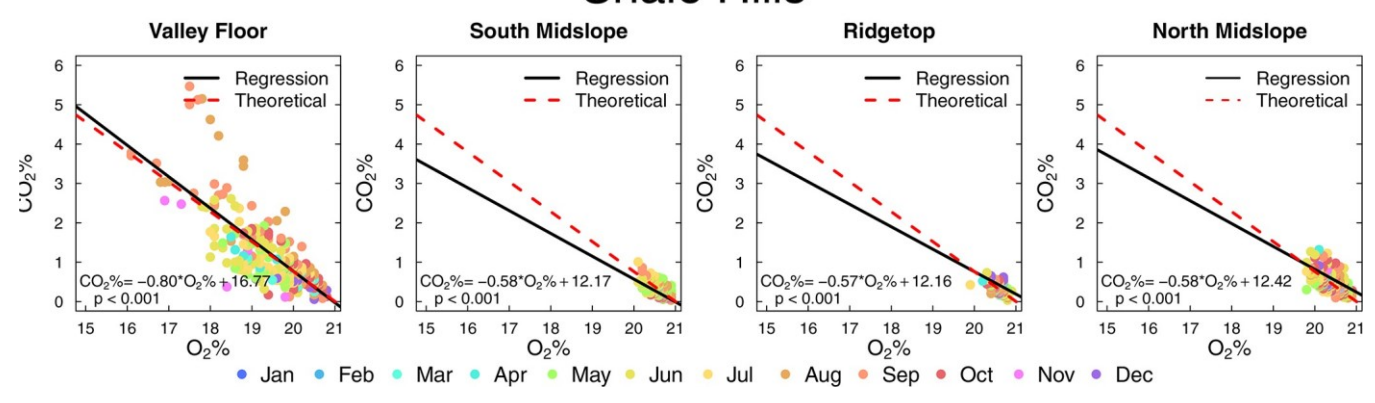


Fig. 5. Plotted pO_2 vs. pCO_2 at the south planar valley floor (SPVF), south midslope (SPMS), ridgetop (SPrt), and north midslope (NPMS) positions in the Shale Hills catchments for August 2015 through November 2017. Point color corresponds to month, the dashed red line corresponds to the theoretical relationship between pO_2 and pCO_2 (ArQ = 1) governed by diffusion and aerobic respiration, with a slope of -0.76 and x-intercept of 21, the black line corresponds to the fitted regression of the data. Slopes that fall below the theoretical relationship (more shallow) indicate systems depleted in CO_2 through carbonate precipitation or silicate weathering, depleted in O_2 through oxidation reactions, or preferential microbial mineralization of lignin and lipid substrates. Slopes that fall above the theoretical relationship (steeper slopes) indicate systems enriched in CO_2 through anaerobic respiration or carbonate weathering and off-gassing or preferential microbial mineralization of organic acid substrates.

Soil Apparent respiratory Quotient

Despite the clear signal of aerobic respiration during the growing season (soil CO_2 decrease and O_2 increase along a slope consistent with the stoichiometry of aerobic respiration), ARQ varies seasonally at both the Shale Hills and Garner Run sites (Fig. 3 and 4). With the exception of the valley floor positions in summer 2016, ARQ is >1 from August to October. Outside of this late growing season period, the ARQ is ≤ 1 . The lowest ARQ (≤ 1) is observed during the late fall and early growing season of the spring. Despite the greater magnitude of seasonal fluctuations in soil gas at depth and at the valley floor hillslope positions, the shift in ARQ with season is observed across all depths and is more distinct at the midslopes and ridgetops of both sites (Fig. 3 and 4). Furthermore, except for during the late growing season

high-ARQ periods, ARQ decreases with depth from near 1 at the soil surface to 0.5 at D-20 (Fig. 3 and 4).

Soil Gas regressions

Regressions of point measurements of pO₂ by pCO₂ by hillslope position (Fig. 5 and 6) provide statistical corroboration of the patterns identified by the interpolated surfaces (Fig. 3 and 4). The ANCOVA test for the effect of hillslope position and lithology indicates a significant effect of lithology (p < 0.001) and hillslope position (p < 0.001) on the slope of the pO₂ by pCO₂ regression line (Table 4). Tukey's HSD post hoc tests indicate that regression slopes are less negative at Shale Hills than at Garner Run. Furthermore, post hoc tests indicate the most negative slopes at the valley floors, followed by ridgetops, north midslopes, and then south midslopes. The differences in slopes

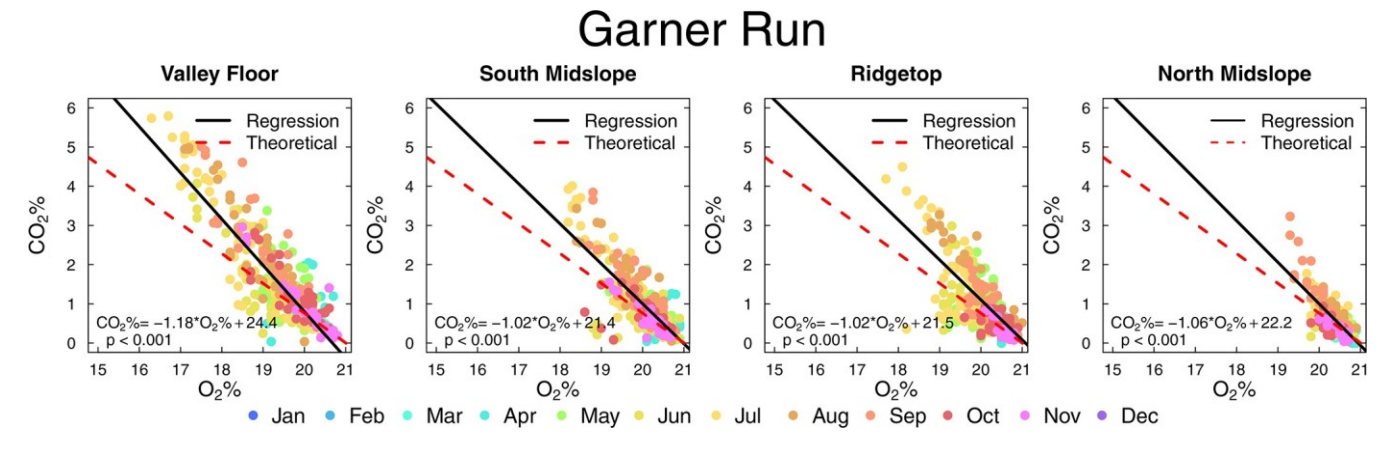


Fig. 6. Plotted pO_2 vs. pCO_2 at the leading ridge Valley Floor (lrVF), leading ridge Midslope (lrMS), leading ridge ridgetop (lrrt), and tussey Mountain Midslope (tMMS) positions in the Garner run (sandstone) catchments for August 2015 through November 2017. Point color corresponds to month, the dashed red line corresponds to the theoretical relationship between pO_2 and pCO_2 (ArQ = 1) governed by diffusion and aerobic respiration, with a slope of -0.76 and x-intercept of 21, the black line corresponds to the fitted regression of the data. Slopes that fall below the theoretical relationship (more shallow) indicate systems depleted in CO_2 through carbonate precipitation or silicate weathering, depleted in O_2 through oxidation reactions, or preferential microbial mineralization of lignin and lipid substrates. Slopes that fall above the theoretical relationship (steeper slopes) indicate systems enriched in CO_2 through anaerobic respiration or carbonate weathering and off-gassing or preferential microbial mineralization of organic acid substrates.

table 4. Analysis of covariance results testing the effect of lithology and hillslope position on the regression slope between soil pCO₂ and pO₂ for all observations. A significant interaction of a factor with O₂ denotes significantly different slopes

Source	df	F	p Value
Lithology	I	90.32	<0.0001
Hillslope position	4	7.45	<0.0001
O ₂	46	86.13	<0.0001
Lithology × O ₂	39	3.71	<0.0001
Hillslope position × O ₂	71	2.753	<0.0001
Lithology × hillslope position × O_2	26	0.4	0.997
Error	2083		

between the lithologies and hillslope positions cannot be attributed to differences in maximum soil depth measured; ANCOVA tests of pO₂ vs. pCO₂ using only data from 40 cm indicate a significant interaction of both hillslope position (p < 0.001) and lithology (p < 0.0001) with pO₂ on pCO₂.

The soil gas regression plots, with point measurements color coded by month, indicate the highest soil pCO₂ and lowest pO₂ in mid- to late summer (July, August, September), with the peak earlier at Garner Run than Shale Hills (Fig. 5 and 6). The ANCOVA results by season indicate that there is a statistically significant shift to more negative regression slopes at all hillslope positions at both Shale Hills and Garner Run in the summer (p< 0.01 at all sites). At Shale Hills, regression slopes for all hillslope positions are not significantly different in the spring and fall (Table 5). In summer those slopes decrease significantly (p< 0.01) and range from –0.7 to –0.9 (Table 5). A similar trend is observed at Garner Run, but the slopes at all sites and in all seasons are higher than at Shale Hills. In spring and fall the Garner run regression slopes range from –0.5 to –0.9, and in summer in summer those slopes decrease significantly, ranging from –1.2 to –1.3 (Table 5).

At the Shale Hills valley floor position, data from August and September show two distinct patterns. In 2016, the data from August and September plot along the theoretical line; this year had a drought throughout the growing season (425 mm precipitation) (Table 6). In 2015 and 2017, the data from August to September plot well above the theoretical line; these years had normal precipitation (750–850 mm precipitation) (Table 6;

table 5. regressions slopes \pm SE of seasonal and growing season soil pO₂ vs. pCO₂ at all hillslope positions in Shale Hills and Garner run.

	Spring (Apr.–June)	Summer (July–Sept.)	Fall (Oct.–Dec.)	All growing seasons
Shale Hills			,	
Valley floor	-0.56 ± 0.08	-0.92 ± 0.06	-0.60 ± 0.07	-0.80 ± 0.04
South midslope	-0.33 ± 0.06	-0.83 ± 0.06	-0.18 ± 0.05	-0.58 ± 0.04
Ridgetop	-0.25 ± 0.14	-0.83 ± 0.08	-0.40 ± 0.06	-0.57 ± 0.05
North midslope	-0.43 ± 0.11	-0.69 ± 0.10	-0.63 ± 0.07	-0.58 ± 0.05
Garner Run				
Valley floor	-0.85 ± 0.08	-1.32 ± 0.05	-1.04 ± 0.07	-I.I7 ± 0.04
South midslope	-0.54 ± 0.07	-1.19 ± 0.06	-0.51 ± 0.08	−1.02 ± 0.04
Ridgetop	-0.50 ± 0.10	-1.18 ± 0.08	-0.48 ± 0.10	−1.02 ± 0.04
North midslope	-0.51 ± 0.07	-1.24 ± 0.08	-0.67 ± 0.07	-1.06 ± 0.05

Fig. 5). These annual differences do not appear in the plots from Garner Run, despite the same sampling years (Fig. 6).

Soil Gas Sensors from Garner Run South Midslope

Soil gas sensors in the south midslope of Garner Run reveal variation in response to freeze-thaw, precipitation, and drying (Fig. 7 and 8). In the winter and early spring, there is little variation in soil pCO₂, and dips in soil pO₂ are consistent with freeze-thaw events (Sánchez-Cañete et al., 2018). The effect of freeze-thaw is most apparent at 30 cm because the response is reduced with depth. At 30 cm, pO₂ is drawn down, pCO₂ increases over the course of the growing season, and the amplitude of pO₂ variation is greater than pCO₂ variation. At 140 cm the pCO₂ variation is still lower in comparison to the pO₂, but the magnitude of difference is not as great as at 30 cm. At 30 cm the seasonal peak in pCO₂ occurs concurrently with the trough in soil pO₂, but at 140 cm the peak and trough are not in sync (Fig. 7). Instead, the pO₂ trough occurs before the peak in pCO₂.

Both gases respond clearly (though not necessarily a 1:1 relationship of consumption/production) to periods of wetting and drying (Fig. 8). For example, after a dry period in June 2017, a precipitation event (denoted with an arrow in Fig. 7 and 8) increased soil pCO₂ and decreased pO₂ at 30 cm, likely by stimulating root and microbial activity. At 140 cm, the intrusion of rainfall enriched in atmospheric air initially increases pO₂ and decreases pCO₂, after which CO₂ increased and O₂ decreased (from mid-June to 1 July), reflecting aerobic respiration. After this initial wetting event, subsequent rainfall events affect soil pCO₂ less than pO₂; pO₂ recovers to the early-June level, whereas pCO₂ remains high (Fig. 8). This same response (stable pCO₂, increasing pO₂) is observed during the rain-free period from mid-August to September (Fig. 8).

DISCussion

Our data indicate that soil pCO₂, pO₂, and ARQ varied seasonally with lithology and hillslope position. Although our results clearly vary with seasonal changes in temperature and soil moisture, as expected based on previous research (e.g., Brook et al., 1983), they are notable because this is the first study to document both soil gases with high temporal and spatial resolution in a humid, temperate forest. Consistent with aerobic respiration, we observed a drawdown

table 6. Monthly precipitation during the growing seasons of 2015, 2016, and 2017. recorded at Shale Hills watershed.

Apr. 101 41.5 May 32.0 91.6 June 186 65.4 July 200 44.8	thly precipitation		
Apr. 101 41.5 May 32.0 91.6 June 186 65.4 July 200 44.8	2016 2	onth 2015	Month
May 32.0 91.6 June 186 65.4 July 200 44.8	mm		
June 186 65.4 July 200 44.8	41.5	pr. 101	Apr.
July 200 44.8	91.6	lay 32.0	May
• •	65.4 I	ne 186	June
Aug. 50.4 47.2	44.8 I	ly 200	July
	47.2	ug. 50.4	Aug.
Sept. 80.3 69.5	69.5	ept. 80.3	Sept.
Oct. 93.5 66	66 I	ct. 93.5	Oct.
Total 743 426	426 8	otal 743	Total

of soil O_2 over the growing season that coincided with increased CO_2 production, and this effect was more pronounced in the valley floor than hillslopes. When accounting for the relationship between pCO_2 and pO_2 , both hillslope position and lithology affected the ARQ calculated from all data points at each catchment (Fig. 5 and 6), and the regression slopes (average ARQ) differed at all sites in the two catchments, indicating a significant effect of lithology.

Most notably, at all hillslope positions and lithologies, the relationship between CO₂ production and O₂ consumption did not always follow the trend predicted by diffusion and aerobic metabolism using carbohydrates (i.e., ARO 1 1). The interpolated surfaces reveal seasonal patterns of ARQ in all sampled sites that are not apparent from the soil O₂ and CO₂ data alone (Fig. 3 and 4). In general, ARQ increased over the growing season to a value >1 in the late summer and decreased to an annual low of <1 in the early growing season. The seasonality of this pattern deviated from previous observations of ARQ <1 reported in both an arid and temperate forest that were attributed to CO₂ dissolution in soil water and Fe oxidation, respectively (Angert et al., 2015; Sánchez-Cañete et al., 2018). We hypothesize that the observation that ARQ >1 at the SSHCZO during the late growing season can be attributed to soil-saturating rainfall events during the growing season. After these events, respiration rates can outstrip the supply of O₂ provided by diffusion; this unmet

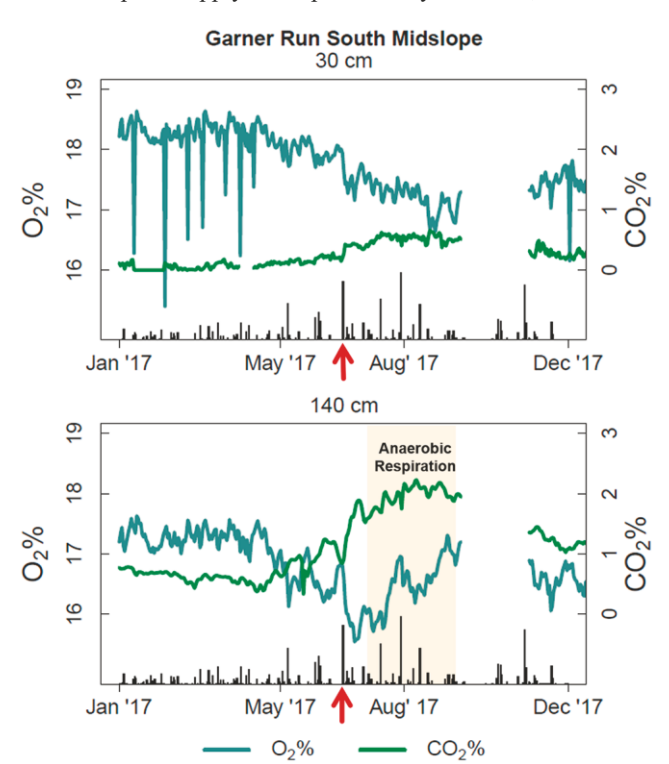


Fig. 7. Day-averaged soil gas plotted with precipitation from 2017 at the south midslope of Garner run. Gaps in data indicate periods when the sensors were not recording. Green lines represent soil pCO_2 , blue lines represent soil pOO_2 , and the black bars represent precipitation events. Volume of water per day is represented by the height of the bars, with the highest bar representing an 80-mm rainfall event. the arrows on the plots indicate the event after which the "period of asynchrony" of soil gas concentrations begins. the tan highlighted area represents a period dominated by anaerobic respiration, suggested by the asynchrony of pCO_2 and pOO_2 .

demand generates reducing microsites of anaerobic respiration that cause the high ARQ we observe in the late growing season.

Hillslope-Position Controls on Soil Gases

In general, the soil pCO₂ is higher and soil pO₂ is lower at the valley floor than other hillslope locations in both Shale Hills and Garner Run (Fig. 3 and 4). This signature at the valley floor positions is likely driven by the wetter soil throughout the growing season, as expected based on the greater accumulating area above the sites (Bergstrom et al., 2016; Jeneso et al., 2010;). Li et al. (2018) report that soil moisture is generally greater at the valley floor position of Shale Hills and Garner Run. Alternating periods of anaerobic respiration (producing CO₂) and abiotic oxidation of metals (consuming oxygen) may be more important at the valley floor hillslope position. Other workers at the SSHCZO have documented soil redox features (Lin et al., 2006) and similar results of more variability in soil O2 (Yesavage et al., 2012) and CO₂ (Hasenmueller et al., 2015; Jin et al., 2014) in the valley floor compared with other hillslope positions in the Shale Hills catchment. Here we document a similar pattern in

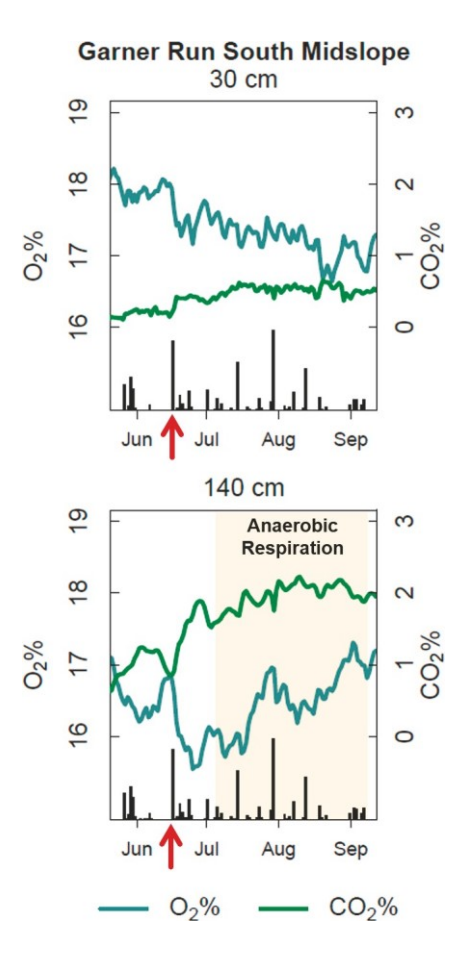


Fig. 8. Day-averaged soil gas from 25 May through 15 September at 30 and 140 cm in the south midslope at Garner run. Green lines represent soil pCO_2 , blue lines represent soil pO_2 , and the black bars represent precipitation events. Volume of water per day is represented by the height of the bars, with the highest bar representing an 80 mm rainfall event. the arrows on the plots indicate the event after which the "period of asynchrony" of soil gas concentrations begins. the tan highlighted area represents a period dominated by anaerobic respiration, suggested by the asynchrony of pCO_2 and pO_2 .

1175

Garner Run, suggesting that these hillslope gradients in ARQ are driven by water and are not limited to one lithology.

lithologic Controls on Soil Gases

Hillslope patterns do not explain all the variation in our data; there are also differences between the Shale Hills and Garner Run sites that cannot be explained by hillslope hydrology. Higher average pCO₂ along the south slope of Garner Run (LRVF, LRMS, LRRT) compared with the south slope of Shale Hills (Table 1), lower pO₂ at LRMS and LRRT than the same sites at Shale Hills (Table 1), and more negative regression slopes (i.e., ARQ >1) of pO₂ vs. pCO₂ at all hillslope positions of Garner Run point to differences in soil physical properties driving soil gas behavior (Fig. 5 and 6). In general, these results indicate that the sandstone sites have greater seasonal fluctuations in soil gases and more negative regression slopes (ARQ >1) more often than shale sites.

Hasenmueller et al. (2015) identified soil porosity, bulk density, and soil depth to be important drivers of pCO2 differences along catenas in the Shale Hills catchment of the SSHCZO. These factors also likely drive differences among lithologies. Shale Hills soils are shallower at equivalent hillslope positions (Lin et al., 2006; Li et al. 2018). However, shallow soils at Shale Hills do not account for all the differences we observed between the two lithologies; when controlling for differences in soil depth, pO₂ is lower and pCO₂ is higher in Garner Run, especially in the late summer (Fig. 3 and 4; Table 2). In the calculation of ARQ, bulk density and tortuosity corrections (effective diffusivity coefficients) are cancelled out, but these factors still affect the rate of diffusion of bulk atmospheric air to deep soils. Soils with higher macroporosity allow for fast gas diffusion (Horn and Smucker, 2005) and therefore could facilitate higher respiration rates at depth in the midslope and ridgetop of Garner Run. Additionally, this porosity allows for faster soil water drainage at Garner Run than Shale Hills. Root density counts at Shale Hills and Garner Run indicate that there are proportionally more roots below 20 cm at Garner Run than at Shale Hills (Li et al., 2018). These roots are likely driven deeper in search of water in the sandier soils of Garner Run (Li et al., 2018), which drives greater CO₂ production and O₂ consumption at depth.

The slopes of the pCO₂ and pO₂ regression lines also suggest that mechanisms of soil gas production and consumption are different between the shale and sandstone site. The regression slopes at Shale Hills are less negative than Garner Run, suggesting a predominance of ARQ >1 at Garner Run and a predominance of ARQ around 1 at Shale Hills (Fig. 2; Table 4). At Garner Run, the slope greater than -0.76 in the midslopes and ridgetop is driven by an increase in pCO₂ relative to O₂ in the late growing season (July, August, and September) (Fig. 2 and 6). This difference cannot be attributed solely to the difference in depth of soil profiles between the lithologies; when only analyzing at 40 cm, a sampling depth common to all hillslope positions, the slopes of the line describing pO₂ vs. pCO₂ are significantly different between Shale Hills and Garner Run. This suggests a seasonal shift to greater CO₂ pro-

duction relative to O_2 consumption from anaerobic respiration in Garner Run during the late growing season.

Continuously recorded pCO₂ and pO₂ Indicate responses to rainfall Events

Sensors indicate day- to week-long variations in soil gas concentrations in response to wetting and drying from precipitation events. Generally, rainfall events correlated with decreased soil O_2 and stimulated CO_2 production (Fig. 7 and 8). This response is not surprising because rainfall has long been documented to decrease soil O_2 by limiting diffusion (Liptzin et al., 2011; Silver et al., 1999). At the same time, increased soil water is also likely to stimulate respiration, which increases CO_2 (Riveros-Iregui et al., 2011).

Our data do not indicate significant CO₂ dissolution in rainwater that others have reported (Ma et al., 2013; Sánchez-Cañete et al., 2018). Although CO₂ is more soluble than O₂ in water, at a pH between 4 and 5 (Hoagland et al., 2017; Li et al., 2018) CO₂ dissolution is limited, and storage of CO₂ in dissolved species would not be favored in the soils of Garner Run (Angert et al., 2015). Instead, we observe that soil O₂ was more responsive than CO₂ to a large rainfall event in June 2017 (Fig. 8). Even amid periods of rainfall and drying, soil CO₂ remains around 2% in the deep soils through September, despite wide fluctuations of >1.5% in O₂ (Fig. 8). The sensors only indicate a response of soil O₂ to drying; as O₂ concentration increases to pre-event levels, CO₂ remains at the post-event level (Fig. 8).

We hypothesize that this pronounced difference between O₂ and CO₂ responses to rainfall during the mid- to late growing season in the subsurface soils is caused by anaerobic microsites within the soil matrix. When soil moisture is high (e.g., after a rainfall event), diffusion is slower and is outpaced by demand for respiration by roots in the subsoils of Garner Run (Li et al., 2018). This short supply of O₂ is most pronounced within soil aggregates whose smaller pores hold water longer than the bulk soil and through which travel paths are longer (Parkin, 1987; Zausig et al., 1993). Under O₂ limitation, heterotrophic microorganisms within the rhizosphere switch to respiration using a different oxidized species, according to thermodynamic favorability and resource availability (Patrick and Jugsujinda, 1992; Peters and Conrad, 1996). The soil sensor data from the growing season of 2017 indicate that despite re-oxygenation of the soil matrix after rainfall, there is still high CO₂ production that does not mirror the change in O₂ as would be predicted based on aerobic respiration/diffusion, pointing to a persistence of reduced microsites and anerobic respiration in the subsurface of LRMS.

Other researchers in temperate forested systems have also observed this signal of anaerobic respiration in the subsurface of upland soils. For example, Hodges et al. (2019) found significant potential for iron respiration in subsurface soils during summer in a forested catchment in the piedmont of South Carolina; the authors attributed this Fe reduction to soil moisture at depth limiting O_2 diffusion in the clayey B horizon during periods of high root respiration. At Shale Hills, Weitzman and Kaye (2018) documented subsurface N_2O production, another pathway

of anaerobic respiration that could generate the observed high CO₂ (relative to O₂) at LRMS. Furthermore, other researchers at Shale Hills found relatively high Fe ($26.7 \pm 3.0 \, \mu \text{mol L}^{-1}$) and Mn ($34.8 \pm 3.2 \, \mu \text{mol L}^{-1}$) in surface waters in early October and comparatively low concentrations in April through June (Herndon et al., 2018). These dissolved metals could be evidence of reductive dissolution in the late growing season. Given these observations in similar systems to Garner Run (deep, wet, subsurface soils) and the presence of oxidized species in the solid-state, like Fe^{III} oxides (Yesavage et al., 2012), it is likely that anaerobic respiration contributes to the CO₂ pool at LRMS.

Controlling Processes for the Seasonality of Soil Gas Chemistry

The signature of lagging CO₂ recovery in the late growing season recorded by the sensors at 140 cm in LRMS is also borne out in the interpolated surfaces from all sites in Garner Run and Shale Hills. At all sites, we observe an increase of ARQ to >1 in the late growing season, consistent with our hypothesis that the high ARQ in the late growing season is caused by anaerobic respiration in reduced microsites that produce CO₂ without consumption of O₂. Further evidence supporting this hypothesis is the lack of ARQ >1 in the dry year of 2016. In 2016, soil moisture was not likely an impediment to O₂ diffusion; reducing microsites did not persist, and therefore ARQ remained closer to values observed in other temperate forests (0.8–1.0) (Angert et al., 2015; Masiello et al., 2008).

Other shifts in soil processes have been identified that could cause ARQ >1 (i.e., factors that increase CO₂ without a decrease in O_2), but they are not likely to be the driving factor of ARQ >1 in this system. The degassing of CO2 from subsurface waters has been identified as a potential mechanism of high ARQ (Angert et al., 2015). However, the carbonate reaction front, where one may assume significant CO₂ in the dissolved phase, in Shale Hills has been identified to coincide with the regional water table (2 m below land surface at the valley and 20 m at the ridges). If degassing of CO₂-rich water significantly contributes to ARQ >1 in the summer, we would anticipate the highest ARQ at the valley floor because the reaction front is shallower and therefore degassed CO₂ would diffuse over a shorter distance (Brantley et al., 2013). The ARQ patterns along the catena suggests the opposite; the highest ARQ is observed at the midslopes and ridgetop (Fig. 3 and 4).

Others have also identified that C substrates with different oxidation states result in different ARQ within the soil system (Randerson et al., 2006). An ARQ >1 could be consistent with a shift from carbohydrate to organic acid consumption by soil heterotrophs (Randerson et al., 2006). However, there is no indication of C substrate limitation that would necessitate a shift to alternate C sources for respiration. Additionally, a decrease in microbial C use efficiency during the late summer could also drive the observed ARQ >1. Higher temperatures, like those in August and September, are correlated with lower C use efficiency (Manzoni et al., 2012). Yet, to account for the observations of ARQ = 1.5, C

use efficiency would need to be half of what it is at other points in the growing season (assuming 50% of soil respiration from heterotrophic microbes [Bhupinderpal-Singh et al., 2003]). Although C substrate and C use efficiency may contribute to the observed pattern, it is likely that anaerobic respiration within low-oxygen microsites drives the observed increase in ARQ.

During the beginning and middle of the growing season, we observe ARQ < 1. We hypothesize that oxidation of reduced metals (facilitated by chemo-lithoautotrophs or through abiotic reactions) in the dissolved phase and parent materials produce this signal of O₂ consumption without CO₂ production. Past researchers at the SSHCZO have recorded evidence of Fe redox cycling and have cultured Fe-oxidizing bacteria from soils sourced throughout the watershed (Yesavage et al., 2012). These Fe oxidizers that thrive in circumneutral pH environments take advantage of thermodynamic gradients at interfaces between low O_2 (where $Fe^{(II)}$ is stable) and higher O_2 (Konhauser et al., 2011). Oxidation of Fe in the early growing season has been well documented at redox transition zones in surface waters of first-order watersheds (Emerson et al., 2010; Fuss et al., 2010; Knorr, 2013). It is also likely that the interior of soil aggregates serve as similar redox gradients, where these Fe-oxidizing bacteria could facilitate oxidation of Fe^(II) in the solid and dissolved phase within aggregates as soil drains through the early growing season. Other oxidation reactions facilitated by chemo-lithoautotrophs could also consume oxygen and produce a signature of ARQ <1. For example, researchers in high-N systems recorded a decrease in soil RQ (respiration quotient, CO₂ produced for O₂ consumed), which they attributed to nitrification (Müller et al., 2004; Tsutsui et al., 2015). However, the effect of nitrification on ARQ is likely negligible at the SSHCZO due to the low potential net nitrification rates found in these watersheds (Weitzman and Kaye, 2018).

Others researchers have attributed ARQ <1 in temperate forest soils to metal oxidation. For example, Angert et al. (2015) observed that forest soils in humid, temperate systems (with low pH) rarely attained the ARQ ?1 anticipated by diffusion and aerobic respiration; they posited that the soils in these acidic forests often have significant levels of reduced Fe in the O and A horizons. Kim et al. (2017) observed a similar signature of Fe redox in the subsurface of a diabase-derived soil in the piedmont of Virginia. This oxidation of Fe in both the soil surface and subsurface likely also contributes to the ARQ <1 we observe in the soils of the SSHCZO because high levels of redox-active metals have been documented in the surface and subsurface soils of Shale Hills (Herndon et al., 2011; Jin et al., 2010; Kraepiel et al., 2015; Yesavage et al., 2012).

Although there are other mechanisms by which the soils at Shale Hills and Garner Run could achieve the observed ARQ <1 in spring (Fig. 2), these are likely to account for a small fraction of the shift we observe. Weathering of carbonate minerals could consume CO₂ (Angert et al., 2015; Ma et al., 2013; Sánchez-Cañete et al., 2018) (Table 1; Fig. 1 and 2). This is probably not the driver of ARQ <1 in the soils of the SSHCZO because the soil pH is too low to support the presence of carbonates and

there is no evidence of carbonates in the subsurface of the Garner Run and Shale Hills sites (Brantley et al., 2018; Li et al., 2018).

Silicate weathering has been documented in the soil of the SSHCZO and accounts for some of the consumed CO_2 in the soils of Garner Run and Shale Hills (Angert et al., 2015; Jin et al., 2014). However, the rate of these weathering reactions is slow, ranging from 0.001 to 0.005 mol Si m $^{-2}$ yr $^{-1}$ (Sullivan et al., 2019), and at most could only consume about 0.3 mg C m $^{-2}$ d $^{-1}$ (Jin et al., 2014). Although model results indicate that the silicate dissolution rate is fastest in the early growing season when we observe ARQ <1, this relatively small consumption potential could not explain our observations. For example, assuming annual soil CO_2 flux of 870 g C m $^{-2}$ yr $^{-1}$ (Shi et al., 2018), silicate weathering rates at Shale Hills would need to be about two orders of magnitude larger (consuming ?30 mg C m $^{-2}$ d $^{-1}$) to account for consumption of CO_2 that shifts ARQ to 0.7.

A change in substrate on which heterotrophs respire during the early growing season or a shift in microbial C use efficiency could cause the observed shift in ARQ (Aon et al., 2001; Dilly, 2001). However, a shift of substrate for heterotrophic respiration to lignin, with a respiratory quotient of about 0.73 (Randerson et al., 2006), could not produce the low ARQ observed because the signal of heterotrophic respiration is muted by autotrophs (mainly roots). Additionally, in open soil systems there is no indication that substrate limitation would shift metabolism to different C sources mid-summer. Therefore, we conclude that oxidation reactions most likely generate the ARQ <1 that we observe in spring at all sites.

In summary, our results provide a seasonal context for the same microsite hypothesis suggested by Angert et al. (2015) to explain ARQ <1 in low-pH forests in the temperate Harvard Forest of Massachusetts and in two alpine forests in Italy. When soil moisture content and respiration rates are high, like after a large rainfall event in the summer, low-oxygen microsites form within aggregates. Heterotrophic microbes within these aggregates shift to terminal electron acceptors other than O2 for respiration and, assuming metal reduction (as opposed to NO₃⁻), generate reduced species that likely stay within the aggregate. By the end of the growing season, the soils of the SSHCZO are nearly saturated and freeze, preventing re-oxidation. Then, as soils warm and dry throughout the spring, the reduced metals are oxidized, consuming newly diffused O₂. The re-oxidized substrates are then ready to be used again by microbes as the lowoxygen microsites are formed again in the summer. This seasonal recycling of soil metals from oxidizing to reducing conditions within soil aggregates ensures the persistence of the ARQ fluctuations over subsequent growing seasons.

Implications: role of Anaerobic respiration in the Carbon Cycle at the Susquehanna Shale Hills Critical Zone Observatory

Measurement of both soil pCO_2 and pO_2 in two lithologies across hillslope positions allows for the calculation of the relative importance of reactions that drive soil ARQ fluctuations as a function of rock type and landscape position. The consumption

of O2 through oxidation of redox-active metals and CO2 through silicate dissolution contribute to the ARO fluctuations that we observe at the SSHCZO, but our measurements and calculations indicate that metal oxidation is a more important seasonal driver than silicate dissolution. This is due to the greater reactivity and higher surface area of metals in the soils of the SSHCZO than the clay minerals and quartz that largely dominate the soils in both rock types. Based on published estimates, silicate weathering at its fastest rate in Shale Hills has the potential to consume about 0.3 mg C m⁻² d⁻¹ (Sullivan et al., 2019). On the other hand, oxidation of 0.1 mmol Fe^(II) kg⁻¹ soil over a month, when assuming the reaction stoichiometry in Table 1, a soil depth of 100 cm, and bulk density of 1.2 g cm⁻³, would consume about 32 mg O_2 m⁻² d⁻¹. This consumption would generate a dip in soil ARQ comparable to a decrease in soil CO₂ flux of 0.32 g C m⁻² d⁻¹. Clearly, metal oxidation at the SSHCZO has the potential to exert a much stronger influence on seasonal soil gas fluctuations than silicate dissolution in these shale- and sandstone-derived soils.

Our measurements also revealed a strong biotic control on ARQ fluctuations. We conclude that a significant fraction of the CO₂ flux in the summer is attributable to anaerobic respiration. In the months of July, August, and September, ARQ is often around 1.5. With an estimated annual soil respiration rate of 870 g C m $^{-2}$ yr $^{-1}$ at the SSHCZO (Shi et al., 2018) and assuming that half of soil respiration is attributable to heterotrophs (Bhupinderpal-Singh et al., 2003) and half of that heterotrophic respiration is anaerobic during the summer (to achieve ARQ of 1.5; Table 1), we calculate that anaerobic respiration contributes about 36 g C m⁻² yr⁻¹ to soil C flux at Shale Hills. This is a low estimate because annual respiration rates do not account for the higher soil respiration in summer and because at some points in the late growing season the ARQ was >1.5. Regardless, this conservative estimate of 36 g C m⁻² yr⁻¹ represents a large C flux from the soil that is not well represented in current soil C models (Keiluweit et al., 2016). Importantly, the signal of anaerobic respiration appears even in well-drained, shallow soils on the ridgetops and midslopes. This suggests that if soils become saturated in summer, respiration will likely outpace diffusion to aggregate interiors, regardless of soil depth.

Under shifting climate regimes, intense storms that saturate soil are anticipated to become more frequent (Greve et al., 2014), and this increased precipitation has been demonstrated to stimulate Fe-reducing conditions, even under bulk oxidizing conditions in soils (Hodges et al., 2018). Therefore, it is likely that under these future rainfall predictions the proportion of anaerobic respiration contributing to total soil C flux will increase (Keiluweit et al., 2016, 2017). This microsite-driven anaerobic respiration is probably not isolated to the SSHCZO and is likely to become ubiquitous during the summer in humid, temperate forests.

ACKNOW | EDGMENtS

Financial support for this work was provided by National Science Foundation Grant EAR-1331726 to S.L.B. for the Susquehanna Shale Hills Critical Zone Observatory. The Shale Hills catchment is located in Penn State's Stone Valley Forest, which is funded by the Penn State

College of Agriculture Sciences, Department of Ecosystem Science and Management, and managed by the staff of the Forestlands Management Office. The Garner Run catchment is located in Rothrock State Forest, which is funded and managed by the Pennsylvania Department of Conservation and Natural Resources, Bureau of Forestry. We thank Brandon Forsythe, Lily Hill, and the rest of the SSHCZO field team for installation of instrumentation and assistance with data collection.

rEFERENCES

- Amundson, R., L. Stern, T. Baisden, and Y. Wang. 1998. The isotopic composition of soil and soil-respired CO₂. Geoderma 82:83–114. doi:10.1016/S0016-7061(97)00098-0
- Angert, A., D. Yakir, M. Rodeghiero, Y. Preisler, E. Davidson, and T. Weiner. 2015. Using O₂ to study the relationships between soil CO2 efflux and soil respiration. Biogeosciences 12:2089–2099. doi:10.5194/bg-12-2089-2015
- Aon, M., D. Sarena, J. Burgos, and S. Cortassa. 2001. Interaction between gas exchange rates, physical and microbiological properties in soils recently subjected to agriculture. Soil Tillage Res. 60:163–171. doi:10.1016/ S0167-1987(01)00191-X
- Bergstrom, A., K. Jencso, and B. McGlynn. 2016. Spatiotemporal processes that contribute to hydrologic exchange between hillslopes, valley bottoms, and streams. Water Resour. Res. 52:4628–4645. doi:10.1002/2015WR017972
- Bhupinderpal-Singh, A. Nordgren, O.M. Löfvenius, M.N. Högberg, P.E. Mellander, and P. Högberg. 2003. Tree root and soil heterotrophic respiration as revealed by girdling of boreal Scots pine forest: Extending observations beyond the first year. Plant Cell Environ. 26:1287–1296. doi:10.1046/j.1365-3040.2003.01053.x
- Brook, G.A., M.E. Folkoff, and E.O. Box. 1983. A world model of soil carbon dioxide. Earth Surf. Process. Landf. 8:79–88. doi:10.1002/esp.3290080108
- Brantley, S.L., R.A. DiBiase, T.A. Russo, Y. Shi, H. Lin, K.J. Davis, et al. 2016. Designing a suite of measurements to understand the critical zone. Earth Surf. Dynam. 4:211–235. doi:10.5194/esurf-4-211-2016
- Brantley, S.L., M.E. Holleran, L. Jin, and E. Bazilevskaya. 2013. Probing deep weathering in the Shale Hills Critical Zone Observatory, Pennsylvania (USA): The hypothesis of nested chemical reaction fronts in the subsurface. Earth Surf. Processes 38:1280–1298. doi:10.1002/esp.3415
- Brantley, S.L., M. Lebedeva, and E. Bazilevskaya. 2014. Relating weathering fronts for acid neutralization and oxidation to pCO₂ and pO₂. In: H.D. Holland and K.K. Turekian, editors, Treatise on geochemistry. 2nd ed. Elsevier, New York. p. 327–352, doi:10.1016/B978-0-08-095975-7.01317-6.
- Brantley, S.L., T. White, N. West, J.Z. Williams, B. Forsythe, D. Shapich, et al. 2018. Susquehanna Shale Hills Critical Zone Observatory: Shale Hills in the context of Shaver's Creek watershed. Vadose Zone J. 17:180092. doi:10.2136/vzj2018.04.0092
- Chadwick, O.A., E.F. Kelly, D.M. Merritts, and R.G. Amundson. 1994. Carbon dioxide consumption during soil development. Biogeochemistry 24:115– 127. doi:10.1007/BF00003268
- Chapin, F.S., III, P.A. Matson, and P. Vitousek. 2011. Principles of terrestrial ecosystem ecology. Springer Science & Business Media, Berlin, Germany. doi:10.1007/978-1-4419-9504-9
- Davidson, E., E. Belk, and R.D. Boone. 1998. Soil water content and temperature as independent or confounded factors controlling soil respiration in a temperate mixed hardwood forest. Glob. Change Biol. 4:217–227. doi:10.1046/j.1365-2486.1998.00128.x
- Dilly, O. 2001. Microbial respiratory quotient during basal metabolism and after glucose amendment in soils and litter. Soil Biol. Biochem. 33:117–127. doi:10.1016/S0038-0717(00)00123-1
- Emerson, D., E.J. Fleming, and J.M. McBeth. 2010. Iron-oxidizing bacteria: An environmental and genomic perspective. Annu. Rev. Microbiol. 64:561– 583. doi:10.1146/annurev.micro.112408.134208
- Fan, Y., M. Clark, D.M. Lawrence, S. Swenson, L.E. Band, et al. 2019. Hillslope hydrology in global change research and Earth system modeling. Water Resour. Res. 55:1737–1772. doi:10.1029/2018WR023903
- Fuss, C.B., C.T. Driscoll, C.E. Johnson, R.J. Petras, and T.J. Fahey. 2010. Dynamics of oxidized and reduced iron in a northern hardwood forest. Biogeochemistry 104:103–119. doi:10.1007/s10533-010-9490-x
- Greve, P., B. Orlowsky, B. Mueller, J. Sheffield, M. Reichstein, and S.I. Seneviratne. 2014. Global assessment of trends in wetting and drying over land. Nat.

- Geosci. 7(10):2247. doi:10.1038/ngeo2247.
- Hasenmueller, E.A., L. Jin, G.E. Stinchcomb, H. Lin, S.L. Brantley, and J.P. Kaye. 2015. Topographic controls on the depth distribution of soil CO2 in a small temperate watershed. Appl. Geochem. 63:58–69. doi:10.1016/j. apgeochem.2015.07.005
- Herndon, E.M., L. Jin, and S.L. Brantley. 2011. Soils reveal widespread manganese enrichment from industrial inputs. Environ. Sci. Technol. 45:241–247. doi:10.1021/es102001w
- Herndon, E.M., G. Steinhoefel, A.L.D. Dere, and P.L. Sullivan. 2018. Perennial flow through convergent hillslopes explains chemodynamic solute behavior in a shale headwater catchment. Chem. Geol. doi:10.1016/j.chemgeo.2018.06.019
- Hoagland, B., T.A. Russo, X. Gu, L. Hill, J. Kaye, B. Forsythe, and S.L. Brantley. 2017. Hyporheic zone influences on concentration-discharge relationships in a headwater sandstone stream. Water Resour. Res. 53:4643–4667. doi:10.1002/2016WR019717
- Hodges, C., E. King, J. Pett-Ridge, and A. Thompson. 2018. Potential for iron reduction increases with rainfall in montane basaltic soils of Hawaii. Soil Sci. Soc. Am. J. 82:176–185. doi:10.2136/sssaj2017.06.0193
- Hodges, C., J. Mallard, D. Markewitz, D. Barcellos, and A. Thompson. 2019. Seasonal and spatial variation in the potential for iron reduction in soils of the Southeastern Piedmont of the US. Catena 180:32–40. doi:10.1016/j. catena.2019.03.026
- Holland, H.D. 1984. The chemical evolution of the atmosphere and oceans. Princeton Univ. Press, Princeton, NJ.
- Holland, H.D., and E.A. Zbinden. 1988. Paleosols and the evolution of the atmosphere: Part I. In: A. Lerman and M. Meybeck, editors, Physical and chemical weathering in geochemical cycles. Springer, Dordrecht, The Netherlands. p. 61–82. doi:10.1007/978-94-009-3071-1_4
- Horn, R., and A. Smucker. 2005. Structure formation and its consequences for gas and water transport in unsaturated arable and forest soils. Soil Tillage Res. 82:5–14. doi:10.1016/j.still.2005.01.002
- Jarecke, K.M., T.D. Loecke, and A.J. Burgin. 2016. Coupled soil oxygen and greenhouse gas dynamics under variable hydrology. Soil Biol. Biochem. 95:164–172. doi:10.1016/j.soilbio.2015.12.018
- Jencso, K.G., B.L. McGlynn, M.N. Gooseff, K.E. Bencala, and S.M. Wondzell. 2010. Hillslope hydrologic connectivity controls riparian groundwater turnover: Implications of catchment structure for riparian buffering and stream water sources. Water Resour. Res. 46:W10524. doi:10.1029/2009WR008818
- Jin, L., R. Ravella, B. Ketchum, P.R. Bierman, P. Heaney, T. White, and S.L. Brantley. 2010. Mineral weathering and elemental transport during hillslope evolution at the Susquehanna/Shale Hills Critical Zone Observatory. Geochim. Cosmochim. Acta 74:3669–3691. doi:10.1016/j.gca.2010.03.036
- Jin, L., N. Ogrinc, T. Yesavage, E.A. Hasenmueller, L. Ma, et al. 2014. The CO2 consumption potential during gray shale weathering: Insights from the evolution of carbon isotopes in the Susquehanna Shale Hills critical zone observatory. Geochim. Cosmochim. Acta 142:260–280. doi:10.1016/j. gca.2014.07.006
- Kaye, J.P., and S.C. Hart. 1998. Restoration and canopy-type effects on soil respiration in a ponderosa pine-bunchgrass ecosystem. Soil Sci. Soc. Am. J. 62(4):1062–1072. doi:10.2136/sssaj1998.03615995006200040030x
- Keiluweit, M., M. Kleber, P. Nico, S. Fendorf, and T. Wanzek. 2017. Anaerobic microsites have an unaccounted role in soil carbon stabilization. Nat. Commun. 8:1771. doi:10.1038/s41467-017-01406-6
- Keiluweit, M., P. Nico, M. Kleber, and S. Fendorf. 2016. Are oxygen limitations under recognized regulators of organic carbon turnover in upland soils? Biogeochemistry 127:157–171. doi:10.1007/s10533-015-0180-6
- Kim, H., G. Stinchcomb, and S.L. Brantley. 2017. Feedbacks among O2 and CO2 in deep soil gas, oxidation of ferrous minerals, and fractures: A hypothesis for steady-state regolith thickness. Earth Planet. Sci. Lett. 460:29–40. doi:10.1016/j.epsl.2016.12.003
- Knorr, K.-H. 2013. DOC-dynamics in a small headwater catchment as driven by redox fluctuations and hydrological flow paths—are DOC exports mediated by iron reduction/oxidation cycles? Biogeosciences 10:891–904. doi:10.5194/bg-10-891-2013
- Konhauser, K.O., A. Kappler, and E.E. Roden. 2011. Iron in microbial metabolisms. Elements 7:89–93. doi:10.2113/gselements.7.2.89
- Kraepiel, A., A. Dere, E. Herndon, and S.L. Brantley. 2015. Natural and anthropogenic processes contributing to metal enrichment in surface soils of central Pennsylvania. Biogeochemistry 123:265–283. doi:10.1007/ s10533-015-0068-5

- Li, L., R.A. DiBiase, J. Del Vecchio, V. Marcon, B. Hoagland, D. Xiao, et al. 2018. The effect of lithology and agriculture at the Susquehanna Shale Hills Critical Zone Observatory. Vadose Zone J. 17:180063. doi:10.2136/ vzj2018.03.0063
- Lin, H., W. Kogelmann, C. Walker, and M. Bruns. 2006. Soil moisture patterns in a forested catchment: A hydropedological perspective. Geoderma 131(3):345–368. doi:10.1016/j.geoderma.2005.03.013
- Liptzin, D., W.L. Silver, and M. Detto. 2011. Temporal dynamics in soil oxygen and greenhouse gases in two humid tropical forests. Ecosystems 14(2):171–182. doi:10.1007/s10021-010-9402-x
- Manzoni, S., P. Taylor, A. Richter, A. Porporato, and G.I. Ågren. 2012. Environmental and stoichiometric controls on microbial carbon-use efficiency in soils. New Phytol. 196(1):79–91. doi:10.1111/j.1469-8137.2012.04225.x
- Masiello, C., M. Gallagher, J. Randerson, R. Deco, and O. Chadwick. 2008. Evaluating two experimental approaches for measuring ecosystem carbon oxidation state and oxidative ratio. J. Geophys. Res. Atmos. 113(G3). doi:10.1029/2007jg000534
- Ma, J., Z.-Y. Wang, B.A. Stevenson, X.-J. Zheng, and Y. Li. 2013. An inorganic CO2 diffusion and dissolution process explains negative CO2 fluxes in saline/alkaline soils. Sci. Rep. 3:2025. doi:10.1038/srep02025
- Müller, C., M.K. Abbasi, C. Kammann, T.J. Clough, R.R. Sherlock, R.J. Stevens, and H. Jäger. 2004. Soil respiratory quotient determined via barometric process separation combined with nitrogen-15 labeling. Soil Sci. Soc. Am. J. 68:1610–1615. doi:10.2136/sssaj2004.1610
- Nychka, D., R. Furrer, J. Paige, and S. Sain. 2017. Fields: Tools for spatial data. University Corporation for Atmospheric Research, Boulder, CO. doi:10.5065/D6W957CT
- Parkin, T.B. 1987. Soil microsites as a source of denitrification variability. Soil Sci. Soc. Am. J. 51:1194–1199. doi:10.2136/sssaj1987.03615995005100050019x
- Patrick, W., and A. Jugsujinda. 1992. Sequential reduction and oxidation of inorganic nitrogen, manganese, and iron in flooded soil. Soil Sci. Soc. Am. J. 56:1071–1073. doi:10.2136/sssaj1992.03615995005600040011x
- Peters, V., and R. Conrad. 1996. Sequential reduction processes and initiation of CH 4 production upon flooding of oxic upland soils. Soil Biol. Biochem. 28:371–382. doi:10.1016/0038-0717(95)00146-8
- R Core Team. 2018. R: A language and environment for statistical computing. R Foundation for Statistical Computing, Vienna, Austria.
- Randerson, J., C. Iello, C. Still, T. Rahn, H. Poorter, and C.B. Field. 2006. Is carbon within the global terrestrial biosphere becoming more oxidized? Implications for trends in atmospheric O2. Glob. Change Biol. 12:260– 271. doi:10.1111/j.1365-2486.2006.01099.x
- Rey, A. 2015. Mind the gap: Non-biological processes contributing to soil CO2 efflux. Glob. Change Biol. 21:1752–1761. doi:10.1111/gcb.12821

- Riveros-Iregui, D.A., B.L. McGlynn, L.A. Marshall, D.L. Welsch, R.E. Emanuel, and H.E. Epstein. 2011. A watershed-scale assessment of a process soil CO₂ production and efflux model. Water Resour. Res. 47. doi:10.1029/2010WR009941.
- Sánchez-Cañete, E.P., G.A. Barron-Gafford, and J. Chorover. 2018. A considerable fraction of soil-respired CO2 is not emitted directly to the atmosphere. Sci. Rep. 8:13518. doi:10.1038/s41598-018-29803-x
- Shi, Y., D.M. Eissenstat, Y. He, and K.J. Davis. 2018. Using a spatially-distributed hydrologic biogeochemistry model with a nitrogen transport module to studythespatialvariation of carbon processes in a Critical Zone Observatory. Ecol. Modell. 380:8–21. doi:10.1016/j.ecolmodel.2018.04.007
- Silver, W., A. Lugo, and M. Keller. 1999. Soil oxygen availability and biogeochemistry along rainfall and topographic gradients in upland wet tropical forest soils. Biogeochemistry 44:301–328. doi:10.1007/BF00996995
- Smith, L.A., D.M. Eissenstat, and M.W. Kaye. 2017. Variability in aboveground carbon driven by slope aspect and curvature in an eastern deciduous forest, USA. Can. J. For. Res. 47:149–158. doi:10.1139/cjfr-2016-0147
- Stinchcomb, G.E., H. Kim, E.A. Hasenmueller, P.L. Sullivan, P.B. Sak, and S.L. Brantley. 2018. Relating soil gas to weathering using rock and regolith geochemistry. Am. J. Sci. 318:727–763. doi:10.2475/07.2018.01
- Sullivan, B.W., T.E. Kolb, S.C. Hart, J.P. Kaye, S. Dore, and M. Montes-Helu. 2008. Thinning reduces soil carbon dioxide but not methane flux from southwestern USA ponderosa pine forests. For. Ecol. Manage. 255:4047– 4055. doi:10.1016/j.foreco.2008.03.051
- Sullivan, P.L., Y. Goddéris, Y. Shi, X. Gu, J. Schott, E.A. Hasenmueller, et al. 2019. Exploring the effect of aspect to inform future earthcasts of climate-driven changes in weathering of shale. J. Geophys. Res. Earth Surf. doi:10.1029/2017JF004556
- Tsutsui, H., T. Fujiwara, D. Inoue, R. Ito, K. Matsukawa, and N. Funamizu. 2015. Relationship between respiratory quotient, nitrification, and nitrous oxide emissions in a forced aerated composting process. Waste Manag. 42:10–16. doi:10.1016/j.wasman.2015.02.038
- Weitzman, J.N., and J.P. Kaye. 2018. Nitrogen budget and topographic controls on nitrous oxide in a shale-based watershed. J. Geophys. Res. Biogeosci. 123. doi:10.1029/2017JG004344.
- Yesavage, T., M.S. Fantle, J. Vervoort, R. Mathur, L. Jin, et al. 2012. Fe cycling in the Shale Hills Critical Zone Observatory, Pennsylvania: An analysis of biogeochemical weathering and Fe isotope fractionation. Geochim. Cosmochim. Acta 99:18–38. doi:10.1016/j.gca.2012.09.029
- Zausig, J., W. Stepniewski, and R. Horn. 1993. Oxygen concentration and redox potential gradients in unsaturated model soil aggregates. Soil Sci. Soc. Am. J. 57:908–916. doi:10.2136/sssaj1993.03615995005700040005x